Chaos and order in a kicked anharmonic oscillator: Classical and quantum analysis

P. Szlachetka and K. Grygiel
Nonlinear Optics Division, Institute of Physics, Adam Mickiewicz University, 60-780 Poznań, Poland

J. Bajer
Laboratory of Quantum Optics, Palacký University, 771 46 Olomouc, Czechoslovakia
(Received 26 January 1993)

The classical dynamics of a kicked anharmonic oscillator is analyzed in terms of Lyapunov exponents. The influence of the quantum corrections on the behavior of the limit cycles and chaotic attractors is considered. Phase portraits are presented. We have shown that quantum corrections destroy chaotic motion even if the system is driven, dissipative, and classically chaotic.

PACS number(s): 05.45.+b, 42.50.Lc

I. INTRODUCTION

In the past decade increasing interest has been devoted to the study modifications introduced by quantum mechanics into the dynamics of classical systems which manifest deterministic chaotic behavior. This problem is frequently referred to as "quantum chaos"—for a review, see Refs. [1,2]. It seems that the simplest and clearest comparison of quantum and classical dynamics is to be found in Wigner's formulation of quantum mechanics—a circumstance well known from quantum optics, where Wigner-like distributions are widely used [3]. This approach makes it possible to treat quantum systems in a "classical way" including all their quantum features and to contrast the quantum and classical dynamics within the framework of a phase picture [4]. The aim of this paper is to study the dissipative classical and quantum dynamics of an anharmonic oscillator driven by a kicked force—a train of pulses. Whereas the case of a coherent driving force is well established [5], that of a train of pulses has not, to our knowledge, been previously applied to the calculation of the dynamical properties of the anharmonic oscillator. Some aspects of the kicked dynamics, however, without damping and in the context of discrete mappings, have been also studied by Berman and Zaslavsky [6]. The quantum anharmonic oscillator plays a significant role in applications not only in quantum optics [5–10] (Kerr effect), but also in quantum statistical physics.

The method used in this paper is similar to that applied by Jensen and Niu [2] for the kicked rotator. However, the difference is that whereas they applied discrete mapping, we study a continuous system (differential equations for the statistic moments) using a Runge-Kutta method.

II. MODEL AND BASIC EQUATIONS

Let us shortly summarize what is well known about the dynamics of an anharmonic oscillator. We write the Hamiltonian in the form [5,9,10]

$$H=H_1+H_2+H_3 , \tag{1}$$

where

$$H_1=\hbar\omega a^\dagger a+\frac{\hbar\chi}{2}a^{\dagger 2}a^2 , \tag{2}$$

$$H_2=i\hbar F(a^\dagger-a) , \tag{3}$$

$$H_3=\hbar\sum_j \Omega_j b_j^\dagger b_j+\hbar\sum_j (K_j b_j a^\dagger+K_j^* b_j^\dagger a) . \tag{4}$$

In the single-mode Hamiltonian H_1, the quantities a ($a^\dagger$) are the photon annihilation (creation) operators, respectively; ω is the frequency of the harmonic oscillator, χ is the anharmonicity parameter. The Hamiltonian H_2 describes the interaction between the classical external driving field F and the single-mode field. The loss mechanism is described by the coupling to a heat bath governed by the reservoir Hamiltonian H_3. Here, the b_j ($b_j^\dagger$) are the boson annihilation (creation) operators of the reservoir. Oscillations with the frequencies Ω_j and K_j are the coupling constants of the interaction with the reservoir. We treat the quantum losses in Louisell's approach [11], that is, on eliminating the reservoir operators we obtain the master equation for the density operator ρ in the form

$$\frac{\partial\rho}{\partial t}=\frac{-i}{\hbar}[H_1+H_2,\rho]+L_{\rm ir}[\rho] . \tag{5}$$

The irreversible term $L_{\rm ir}[\rho]$ describes damping and has the form

$$L_{\rm ir}=\frac{\gamma}{2}(2a\rho a^\dagger-a^\dagger a\rho-\rho a^\dagger a)+\gamma\langle n\rangle(a^\dagger\rho a+a\rho a^\dagger-a^\dagger a\rho-\rho aa^\dagger) . \tag{6}$$

The parameter γ is the damping constant, and $\langle n\rangle$ is the mean number of reservoir photons. The quantum theory of damping [11] assumes that the reservoir spectrum is flat, so the mean number of reservoir oscillators $\langle n\rangle=\langle b_j^\dagger(0)b_j(0)\rangle=[\exp(\hbar\omega/kT)-1]^{-1}$ in the jth mode is independent of j. Thus, the reservoir oscillators form a thermal system. The case $\langle n\rangle=0$ corresponds to vacuum fluctuations (zero-temperature heat bath). It is convenient to consider the quantum dynamics of the system (1)–(4) in the interaction picture. Then the master

equation for the density operator ρ is given by [8,10]

$$\frac{\partial\rho}{\partial\tau}=-i[\tfrac{1}{2}a^{\dagger 2}a^2+i\mathcal{F}(a^\dagger-a),\rho]+\frac{\Gamma}{2}(2a\rho a^\dagger-a^\dagger a\rho-\rho a^\dagger a)+\Gamma\langle n\rangle(a^\dagger\rho a+a\rho a^\dagger-a^\dagger a\rho-\rho aa^\dagger)\ , \tag{7}$$

where $\tau=t\chi$ is the redefined time, $\Gamma=\gamma/\chi$, and $\mathcal{F}=F/\chi$. The Hamiltonian $\hbar\omega a^\dagger a$ does not appear in Eq. (7) as a consequence of the interaction picture.

The above master equation can be transformed, applying Louisell's technique [11], to a c-number partial differential equation. Three kinds of equations can be derived from (7). First, an equation for the Wigner function $\Phi_{(\mathrm{sym})}$ related to symmetric (Weyl) ordering of the field operators $a,a^\dagger$; second, an equation for the Wigner-like function $\Phi_{(A)}$ related to antinormal ordering of the operators; and third, an equation for the Wigner-like function Φ_N related to normal ordering. The statistical properties of the Φ functions are discussed fully in the book by Peřina [3]. These are quasidistribution functions in the complex plane (α,α^*), where the quantity α is an eigenvalue of the annihilation operator a, i.e., $a|\alpha\rangle=\alpha|\alpha\rangle$. Here, $|\alpha\rangle$ is a coherent state.

For convenience we introduce the so-called s ordering of the field operators $a,a^\dagger$. Then we can write $\Phi_{(\mathrm{sym})}=\Phi_{(0)}$, $\Phi_{(A)}=\Phi_{(-1)}$, and $\Phi_{(N)}=\Phi_{(1)}$.

From (7) we get the generalized Fokker-Planck equation for the quasidistribution $\Phi_{(s)}(\alpha^*,\alpha;\tau)$ related to the s ordering [10]:

$$\frac{\partial\Phi_{(s)}}{\partial\tau}=K+Q\ , \tag{8}$$

where

$$K=\frac{\partial}{\partial\alpha}[(\tfrac{1}{2}\Gamma\alpha-\mathcal{F}+i\alpha|\alpha|^2)\Phi_{(s)}]+\frac{\partial}{\partial\alpha^*}[(\tfrac{1}{2}\Gamma\alpha^*-\mathcal{F}-i\alpha^*|\alpha|^2)\Phi_{(s)}]+\Gamma\langle n\rangle\frac{\partial^2}{\partial\alpha\partial\alpha^*}\Phi_{(s)}\ ,$$

$$Q=-i\left[(1-s)\frac{\partial}{\partial\alpha}\alpha\Phi_{(s)}-(1-s)\frac{\partial}{\partial\alpha^*}\alpha^*\Phi_{(s)}+\frac{s}{2}\frac{\partial^2}{\partial\alpha^2}\alpha^2\Phi_{(s)}-\frac{s}{2}\frac{\partial^2}{\partial\alpha^{*2}}\alpha^{*2}\Phi_{(s)}+\frac{(s^2-1)}{4}\frac{\partial^3}{\partial\alpha^{*2}\partial\alpha}\alpha^*\Phi_{(s)}-\frac{(s^2-1)}{4}\frac{\partial^3}{\partial\alpha^2\partial\alpha^*}\alpha\Phi_{(s)}\right]+\Gamma\frac{(1-s)}{2}\frac{\partial^2}{\partial\alpha\partial\alpha^*}\Phi_{(s)}\ . \tag{9}$$

Let us emphasize that there is no difference among the equations for $\Phi_{(\mathrm{sym})}$, $\Phi_{(A)}$, and $\Phi_{(N)}$ as long as the system (1)–(4) is classical. This problem has been studied in [5,7]. In the classical limit the term Q in Eq. (8) vanishes and $\Phi_{(s)}$ is a classical distribution function [5]. For $Q=0$ and $\Gamma=0$, Eq. (8) reduces to the classical Liouville equation, and for $Q=0$ and $\Gamma\neq0$ to the classical Fokker-Planck equation. So, we can say that the K term governs classical dynamics whereas the Q term adds the quantum (operator) correction. The decision as to whether chaos does or does not appear in the system (1)–(4) can be made by investigating the separation rate of two peaks of a $\Phi_{(s)}$ function initially close to each other or by the analysis of equations for the statistical moments originating in Eq. (8). Thus, instead of attempting to solve the partial differential equation (8) we deal with the problem of solving a set of ordinary differential equations for the statistical moments.

III. TRUNCATION SCHEME

A. Statistical moments

The calculation of statistical moments with the help of $\Phi_{(s)}$ is simple. For example, if we want to calculate the average number of photons $\langle a^\dagger a\rangle$ we use one of three functions $\Phi_{(N)}$, $\Phi_{(A)}$, or $\Phi_{(\mathrm{sym})}$. We have

$$\langle a^\dagger a\rangle=\int\alpha^*\alpha\Phi_{(N)}(\alpha^*,\alpha)d^2\alpha\ , \tag{10}$$

$$\langle a^\dagger a\rangle=\int(\alpha^*\alpha-1)\Phi_{(A)}(\alpha^*,\alpha)d^2\alpha\ , \tag{11}$$

$$\langle a^\dagger a\rangle=\int(\alpha^*\alpha-\tfrac{1}{2})\Phi_{(\mathrm{sym})}(\alpha^*,\alpha)d^2\alpha\ . \tag{12}$$

The value of $\langle a^\dagger a\rangle$ is always the same but the averaging procedure differs in each case. The relations (10)–(12) are a simple consequence of the boson commutation relation $[a,a^\dagger]=1$ and the definition

$$\langle\alpha^*\alpha\rangle_{(s)}=\int\alpha^*\alpha\Phi_{(s)}(\alpha^*,\alpha)d^2\alpha\ , \tag{13}$$

where $\langle\alpha^*\alpha\rangle_{(N)}=\langle a^\dagger a\rangle$, $\langle\alpha^*\alpha\rangle_{(A)}=\langle aa^\dagger\rangle$, and $\langle\alpha^*\alpha\rangle_{(\mathrm{sym})}=\frac{1}{2}\langle a^\dagger a+aa^\dagger\rangle$. It is obvious that some expectation values do not depend on ordering, for example $\langle a^{\dagger n}\rangle=\langle\alpha^{*n}\rangle_{(N)}=\langle\alpha^{*n}\rangle_{(A)}=\langle\alpha^{*n}\rangle_{(\mathrm{sym})}$.

The function $\Phi_{(s)}$ allows us to define the quantum cumulants. The cumulants of first order are given by

$$\langle\alpha^*\rangle_{(s)}=\xi^*,\quad\langle\alpha\rangle_{(s)}=\xi\ . \tag{14}$$

The cumulants of second order have the forms

$$\langle\alpha^*\alpha\rangle_{(s)}-\langle\alpha^*\rangle_{(s)}\langle\alpha\rangle_{(s)}=B_{(s)}\ , \tag{15}$$

$$\langle\alpha^{*2}\rangle_{(s)}-\langle\alpha^*\rangle_{(s)}^2=C^*,\quad\langle\alpha^2\rangle_{(s)}-\langle\alpha\rangle_{(s)}^2=C\ . \tag{16}$$

It is easy to note that simple relations hold among $B_{(N)}$, $B_{(A)}$, and $B_{(\mathrm{sym})}$, namely, $B_{(A)}=B_{(N)}+1$ and $B_{(\mathrm{sym})}=\frac{1}{2}(2B_{(N)}+1)$. Thus the average number of photons can be expressed with the help of s ordering as follows: $\langle a^\dagger a\rangle=G_{(s)}+\xi^*\xi$, where $G_{(s)}=B_{(s)}-(1-s)/2$.

The Fokker-Planck equation (8) generates an infinite and hierarchic set of equations for the statistical moments. In this paper we restrict ourselves to the second

truncation, i.e., to the equations for ξ, C, and $G_{(s)}$. We arrive at the following set of equations (see Appendix):

$$\frac{d\xi}{d\tau}=-\tfrac{1}{2}\Gamma\xi+\mathcal{F}-i[2G_{(s)}\xi+C\xi^*+\xi^2\xi^*]\ , \tag{17}$$

$$\frac{dC}{d\tau}=-\Gamma C-i[\xi^2(1+2G_{(s)})+C(1+4|\xi|^2)] -6iG_{(s)}C\ , \tag{18}$$

$$\frac{dG_{(s)}}{d\tau}=-\Gamma G_{(s)}+i[C\xi^{*2}-C^*\xi^2]+\Gamma\langle n\rangle\ . \tag{19}$$

The above set consists of five equations in the real variables Reξ, Imξ, ReC, ImC, and $G_{(s)}$.

B. First truncation—classical limit

The physical sense of the truncation is clear if we note that the first truncation ($C=G_{(s)}=0$) gives only the classical equation for the anharmonic oscillator

$$\frac{d\xi}{d\tau}=-\tfrac{1}{2}\Gamma\xi+\mathcal{F}(\tau)-i\xi^2\xi^*\ . \tag{20}$$

Thus, $\langle a^\dagger a\rangle=|\xi|^2$ is a classical intensity. The system (20) is nonautonomous if the function $\mathcal{F}$ is explicitly time dependent. The autonomized version of Eq. (20) is given by

$$\frac{d\xi}{d\tau}=-\tfrac{1}{2}\Gamma\xi+\mathcal{F}(w)-i\xi^2\xi^*\ ,$$
$$\frac{dw}{d\tau}=1,\quad w(0)=0\ . \tag{21}$$

It is readily seen that the set of equations (21) consists of three equations of motion in the real variables Reξ, Imξ, w. It is well known that chaos in autonomous systems can appear only if the number of equations is equal to three or greater. Therefore, if $\mathcal{F}(\tau)=$const, chaos in the system does not appear since the set (21) becomes a two-dimensional autonomous system. The driving field is in the form of a train of rectangular computer-simulated pulses. The length of the pulse is denoted by T_1, whereas T_2 is the distance between the pulses, and $\mathcal{F}_0$ is their height. The time evolution between two kicks is governed by the dissipative dynamics ruled by $H=H_1+H_3$. For $T_2=0$ the train of pulses becomes a coherent driving field.

We examine the dynamics of the system (20) with the initial conditions $\xi(0)=1+i$. Moreover, we put $\Gamma=0.5$, $\mathcal{F}_0=2$, $T_2=1$, and $0<T_1<7.5$. To identify order and chaotic behavior of a nonautonomous system we usually use its autonomized version. The spectrum of Lyapunov exponents for a three-dimensional autonomized system like (21) has a Lyapunov spectrum of the type $\{\lambda_1,\lambda_2,\lambda_3=0\}$. It can be calculated adopting the procedure proposed by Wolf *et al.* [12]. Wolf's procedure works well if the function $F(w)$ possesses its first derivative at any point. This requirement is not well satisfied in our case, where the function $F(w)$ is in the form of sharp pulses. However, the existence of the first derivative of $F(\tau)$ is not necessary if the dynamical system remains nonautonomous [13]. Then the number of Lyapunov exponents reduces from three $\{\lambda_1,\lambda_2,0\}$ to two $\{\lambda_1,\lambda_2\}$ [14]. We have the following (nonautonomized) spectra: a chaotic attractor $\{+,-\}$, a quasiperiodic orbit $\{0,-\}$, and a limit cycle or fixed point $\{-,-\}$. Therefore, in this notation there is no difference between a limit cycle and a fixed point.

The spectrum of Lyapunov exponents for the system (20) plotted versus the pulse duration T_1 is presented in Fig. 1. We note that by fluently varying the length of the pulse T_1 we turn order into chaos and chaos into order. For $0<T_1<0.84$ and $1.08<T_1<7.5$ the maximal Lyapunov exponents λ_1 are negative or equal to zero and, in consequence, lead to limit cycles and quasiperiodic orbits. In the points where $\lambda_1=0$ the system switches its periodicity. By way of example, this takes place near $T_1=0.7$. For $T_1=0.65$ and $T_1=0.75$ we observe two limit cycles in the phase space (Reξ,Imξ) with the Lyapunov spectra $\{-0.36,-0.36\}$ and $\{-0.36,-0.37\}$, respectively. The difference is that the first limit cycle is related to one-period oscillations in the intensity $|\xi|^2$ whereas the second limit cycle is related to two-period oscillations.

It is interesting to note that the region $1.08<T_1<7.5$ is reached in multiperiod oscillations of the intensity $|\xi|^2$. For $T_1=6$ we observe a limit cycle (Fig. 2, solid line) which is related to three-period oscillations of the intensity. This is shown in Fig. 3 (solid line). The Lyapunov exponents are $\{-0.20,-0.52\}$.

For $T_1=1.56$ we observe four-period oscillations of the intensity $|\xi|^2$. In this case the spectrum of Lyapunov exponents is given by $\{-0.06,-0.66\}$. The limit cycle for $T_1=1.56$ is shown in Fig. 4(a) and the four-period oscillations of the intensity in Fig. 5(a).

Chaos appears only in the region $0.85<T_1<1.08$ and is maximal for $T_1=0.98$. Then the Lyapunov spectrum is $\{0.30,-1.02\}$. The case with $T_1=0.98$ is illustrated

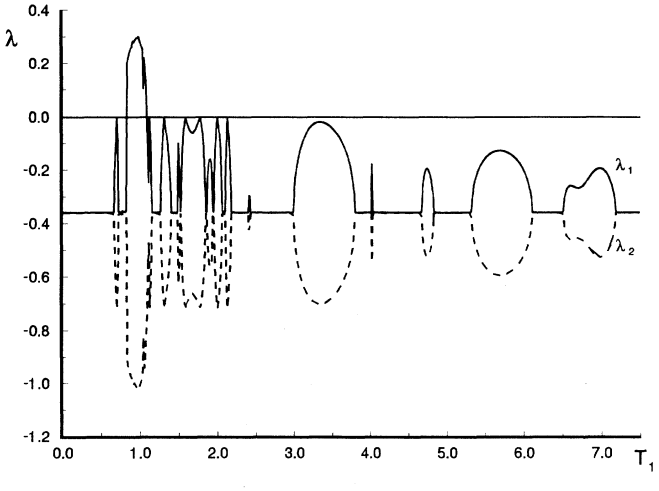

FIG. 1. Spectrum of Lyapunov exponents λ_1,λ_2 for the nonautonomous system (20) plotted vs the pulse duration $0\le T_1\le 7.5$ for $T_2=1$, $\mathcal{F}_0=2$, $\Gamma=0.5$, and $\xi(0)=1+i$. The classical case.

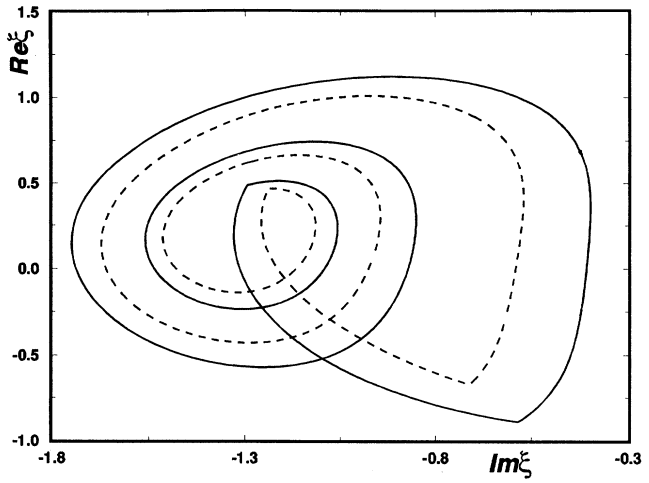

FIG. 2. Phase portraits Reξ vs Imξ. Limit cycles. Solid line, the classical case; Eq. (20) with the initial condition $\xi(0)=1+i$. The parameters of the pulse are $T_1=6$, $T_2=1$, and $\mathcal{F}_0=2$. The damping constant is $\Gamma=0.5$ and $100<\tau<200$. Dashed line, the quantum system; Eqs. (17)–(19) with the initial conditions $\xi(0)=1+i$ and $G_{(s)}(0)=C(0)=0$. The parameters of the pulse are $T_1=6$, $T_2=1$, and $\mathcal{F}_0=2$. The damping constant is $\Gamma=0.5$ and $100<\tau<200$.

in Figs. 6(a) and 7(a). The phase point is seen to plot a typical chaotic trajectory. The intensity $|\xi|^2$ behaves similarly, varying chaotically in the course of time.

The situation presented in the above figures changes dramatically if, instead of Eq. (20), its quantum version Eqs. (17)–(19) is taken into account.

C. Second truncation — quantum correction

The dynamics of the nonautonomous system (17)–(19) including the quantum corrections is governed by five Lyapunov exponents (five equations in real variables). Our system is studied with $\langle n \rangle=0$ and the initial conditions $\xi(0)=1+i$ and $G_{(s)}(0)=C(0)=0$. The spectrum of Lyapunov exponents $\{\lambda_1,\lambda_2,\lambda_3,\lambda_4,\lambda_5\}$ plotted versus the pulse duration T_1 is presented in Fig. 8. Here, λ_1 is the maximal Lyapunov exponent, and is negative in contradistinction to Fig. 1. Therefore the chaotic oscillations due to quantum corrections vanish, and the regular oscillations remain regular but change their structure.

After quantum correction the geometry of the limit cycle for $T_1=6$ remains unchanged, albeit its "volume" (basin of attraction) is reduced. This is visualized in Fig. 2 (dashed line). The values of the Lyapunov exponents for the "reduced" limit cycle are $\{-0.17, -0.56, -0.66, -0.66, -0.84\}$. The maximal Lyapunov exponents before and after the quantum correction satisfy the relation $\lambda_1^{\text{class}}<\lambda_1^{\text{quant}}$. The quantum correction moreover reduces the oscillations of the intensity. The three-periodic oscillations (Fig. 3, solid line) remain three-periodic but their amplitude is reduced (Fig. 3, dashed line).

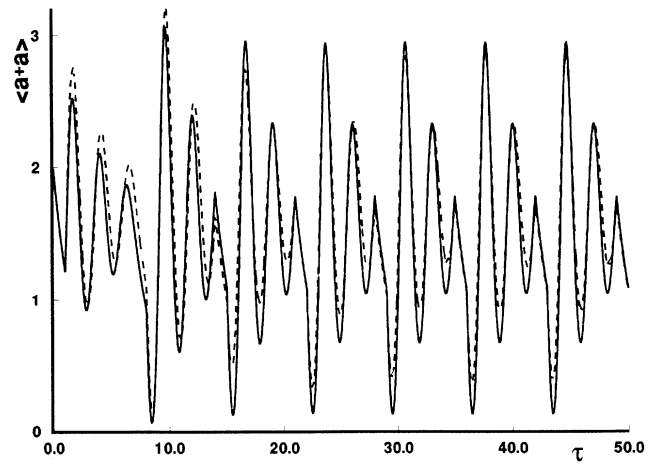

FIG. 3. Time evolution of the classical (solid line) and quantum (dashed line) intensities for the parameters of Fig. 2.

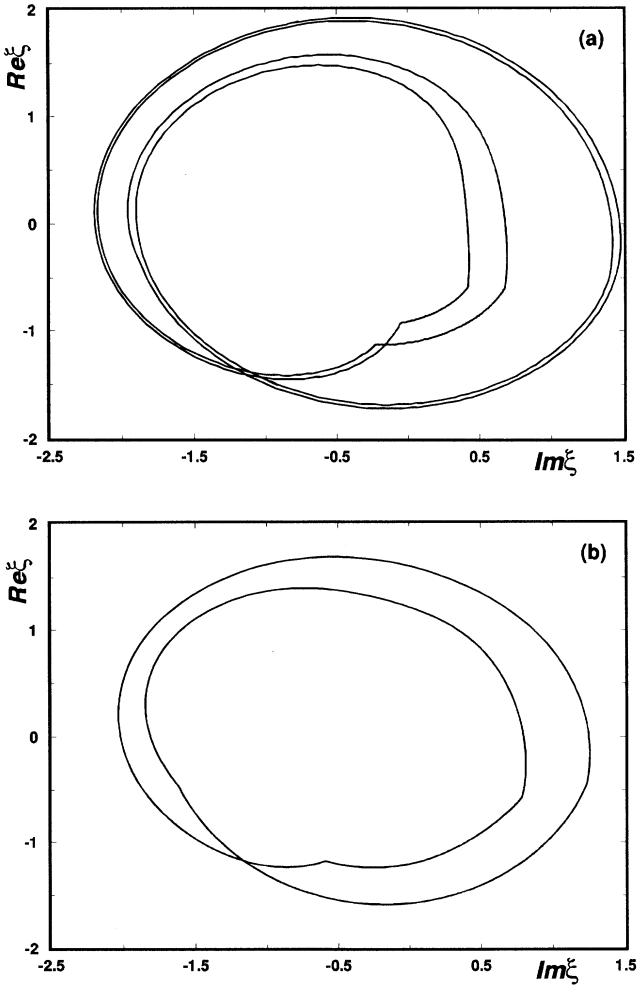

FIG. 4. Same as in Fig. 2 but for $T_1=1.56$, $T_2=1$, $\mathcal{F}_0=2$, $\Gamma=0.5$; (a) shows the limit cycle for the classical system, (b) shows the same limit cycle after the quantum correction.

It is interesting to note that after quantum correction for some cases we can also observe a reduction of periodicity. For example, in the case of $T_1=1.56$ the four-period oscillations [Figs. 4(a) and 5(a)] in the quantum version become two-periodic [Figs. 4(b) and 5(b)]. As is seen the geometry of the limit cycles before and after the quantum correction differs strongly. The Lyapunov exponents for the quantum case presented in Figs. 4(b) and 5(b) are $\{-0.18,-0.19,-0.77,-0.77,-0.97\}$. Obviously $\lambda_1^{\text{class}}>\lambda_1^{\text{quant}}$.

The chaotic trajectory [Fig. 6(a)] is now a periodic trajectory [Fig. 6(b)], and the chaotic oscillations of the intensity [Fig. 7(a)] change into four-period oscillations [Fig. 7(b)]. The Lyapunov exponents now become $\{-0.15,-0.53,-0.53,-0.76,-0.91\}$. We have $\lambda_1^{\text{class}}>0$ and $\lambda_1^{\text{quant}}<0$. Let us emphasize that a similar transition from chaos to order has been found by Jensen and Niu [2] for the quantum kicked rotator.

D. Third truncation

The question is what happens if third-order or higher-order corrections are taken into account? Let us note that the set (17)–(19) consists of five equations in real variables. If third-order truncation is performed, the set (17)–(19) is additionally modified and supplemented with four equations in real variables thus leading to nine equations. The fourth truncation leads to 15 equations in real variables, etc. From the formal point of view, the quantum corrections become more and more rigorous with higher and higher order of the approximation. On the other hand, even if the numerical calculations are performed in extended precision, computer errors can accumulate significantly leading to spurious high-order quantum corrections due to the increasing numbers of equations and iterations. We have estimated that the second truncation gives a quantum correction to the classical solution, whereas third truncation gives only a 0.2% correction. Therefore, the third-order correction is relatively small and has been neglected. Moreover, we cannot obtain an integral of motion in this case (energy is nonconserved).

Let us emphasize that there is yet a stronger argument which causes that the third-order truncation is artificial

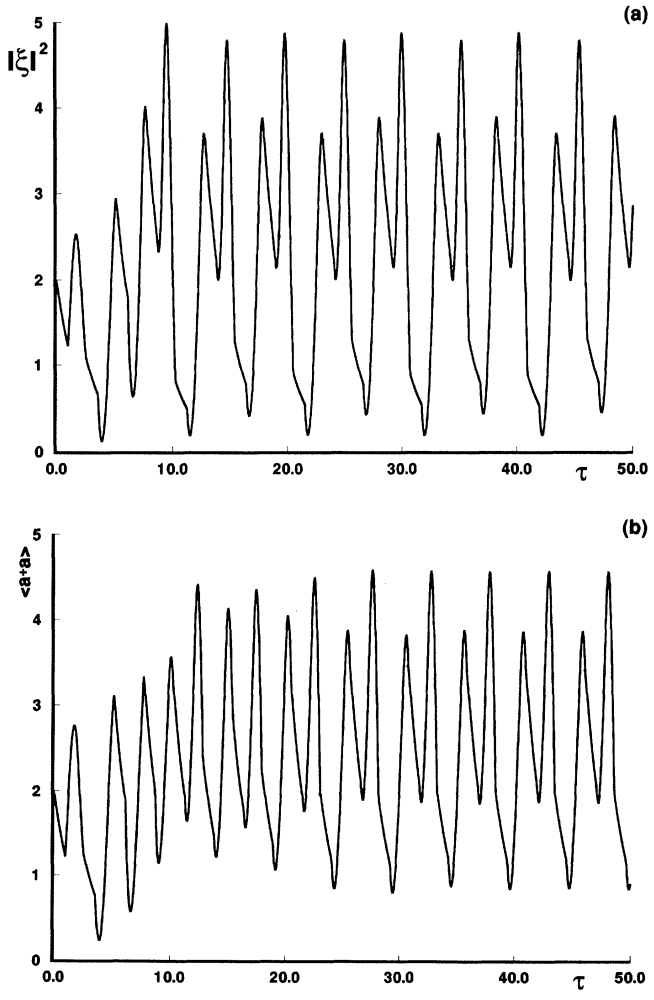

FIG. 5. Time evolution of the classical (a) and quantum (b) intensities for the parameters of Fig. 4.

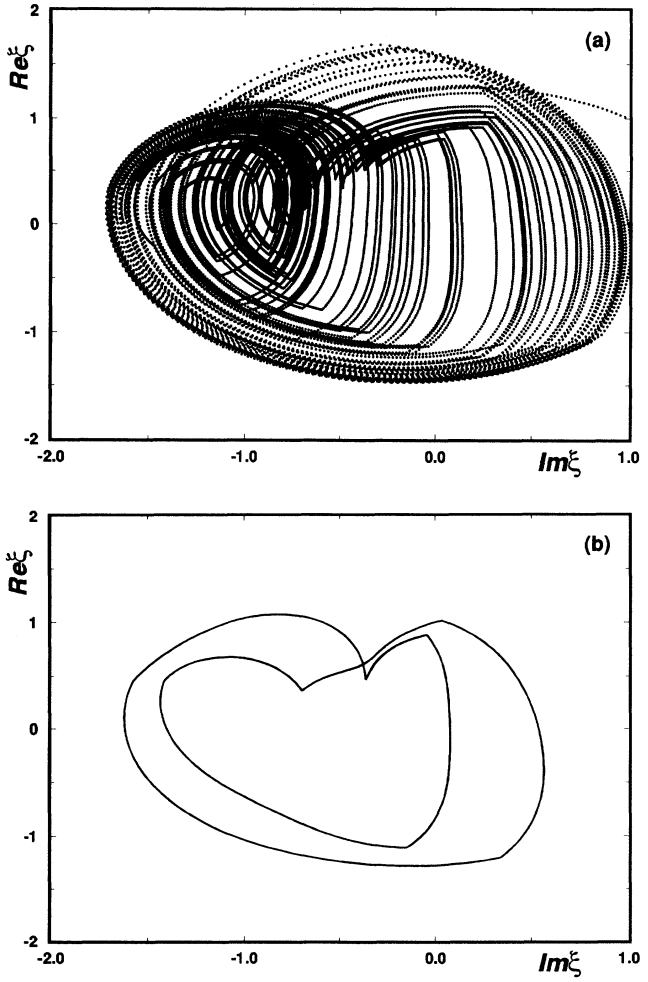

FIG. 6. Same as in Fig. 2 but for $T_1=0.98$, $T_2=1$, $\mathcal{F}_0=2$, $\Gamma=0.5$, $\xi(0)=1+i$, and $G_{(s)}(0)=C(0)=0$; (a) is the classical chaotic orbit, (b) is the same orbit after quantum correction.

rather than systematic as proved by Pawula [15] on the basis of a theorem proposed by Marcinkiewicz [16]. This theorem leads to the conclusion that the function $\Phi_{(s)}$ (for all s) with a finite cumulant expansion cannot be positive if the order of the highest nonvanishing cumulant is greater than 2. Therefore it appears illogical to truncate an infinite and hierarchic set of equations for cumulants retaining a finite number of the equations for cumulants higher than 3.

IV. CONCLUDING REMARKS

In this paper we have studied the quantum and classical dynamics of a dissipative anharmonic oscillator driven by a train of pulses. We have shown that chaotic behavior of the classical system—at a particular set of parameter values—disappears in the quantum case. For the quantum system the maximal Lyapunov exponent is always negative in contradistinction to the classical system. This is obvious from Fig. 9. And, moreover, Fig. 9 shows explicitly that the quantum correction does not shift classical chaos to different regions of the parametric space.

There are regions for the classical system where the maximal Lyapunov exponent is negative, pointing to ordered motion. In this case, after quantum correction, the maximal Lyapunov exponent changes its value albeit remaining negative. Therefore the system maintains its ordered behavior, but the limit cycles change their basins of attraction. For some cases we also observe changes in the periodicity of intensity. Generally, the symmetry of the Lyapunov exponents λ_1, λ_2 for the classical system (Fig. 1) is perturbed by the quantum correction [Fig. 8(a)]—but the crucial result resides in the elimination of the region of chaos. This fact can provide the back-

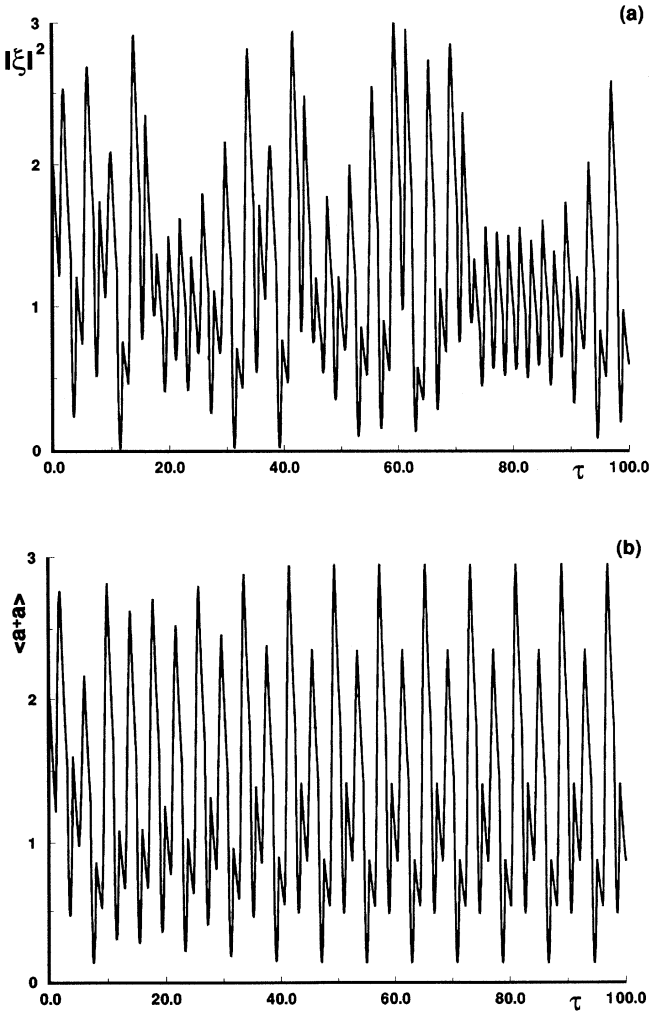

FIG. 7. Time evolution of the classical (a) and quantum (b) intensities for the parameters of Fig. 6. The intensity $|\xi|^2$ evolves from chaotic oscillations, in the classical limit, to four-period oscillations after quantum correction.

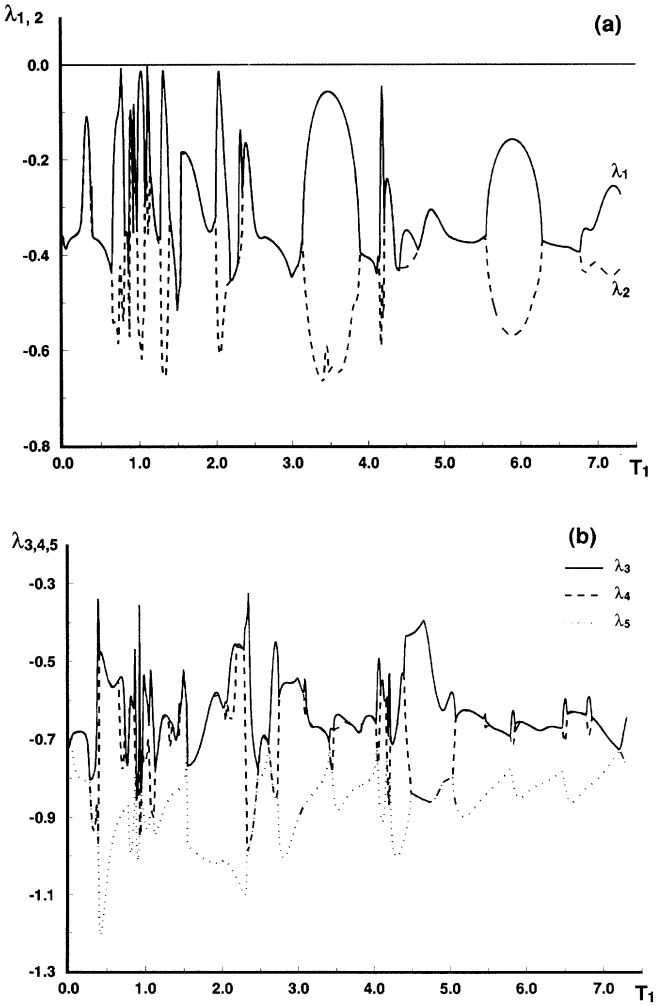

FIG. 8. Spectrum of Lyapunov exponents λ_1, λ_2, λ_3, λ_4, and λ_5 for the nonautonomous system (17)–(19) plotted vs the pulse duration $0 \le T_1 \le 7.5$ for $T_2 = 1$, $\mathcal{F}_0 = 2$, $\Gamma = 0.5$. The initial conditions are $\xi(0) = 1 + i$, $G_{(s)}(0) = 0$ and $C(0) = 0$. Figure (a) presents the same Lyapunov exponents as in Fig. 1 but after the quantum corrections. Figure (b) shows the other exponents λ_3, λ_4, and λ_5.

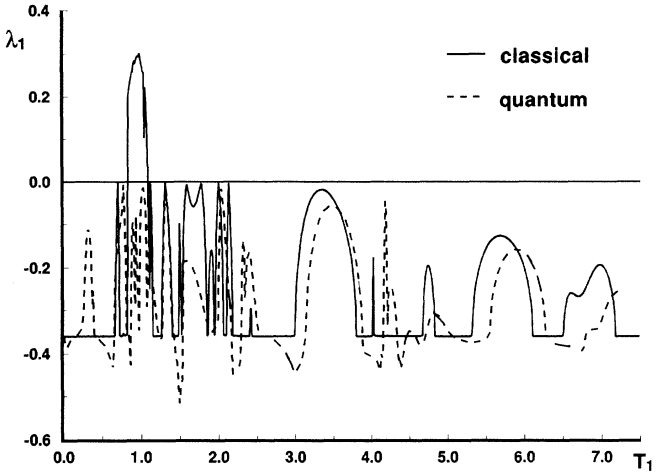

FIG. 9. Maximal Lyapunov exponents for the system before (solid line) and after quantum correction (dashed line). See Figs. 1 and 8(a).

ground for the further experimental verifications of the quantum theory.

In Ref. [17] Ford and Ilg have proved that the time evolution of finite, bounded, undriven quantum systems is nonchaotic. We conclude with the following statement: we have found an example of a system which is driven, dissipative, and at the same time chaotic in its classical description—but its quantum treatment leads to nonchaotic motion.

ACKNOWLEDGMENTS

We are very grateful to Professor Peřina for his helpful discussion. This work was partially supported (J.B.) within the framework of a Palacký University Grant.

APPENDIX: THE DERIVATION OF EQS. (17)–(19)

Let us start with the definition of the statistical moments

$$\langle \alpha^{*m}\alpha^n\rangle_{(s)}=\int \alpha^{*m}\alpha^n\Phi_{(s)}(\alpha^*,\alpha)d^2\alpha\ , \tag{A1}$$

where $d^2\alpha=d(\mathrm{Re}\alpha)d(\mathrm{Im}\alpha)$. Therefore, the equation of motion for $\langle \alpha^{*m}\alpha^n\rangle_{(s)}$ is given by

$$\frac{d}{d\tau}\langle \alpha^{*m}\alpha^n\rangle_{(s)}=\int \alpha^{*m}\alpha^n\frac{d\Phi_{(s)}(\alpha^*,\alpha)}{d\tau}d^2\alpha\ . \tag{A2}$$

If we use Eq. (8) for $d\Phi_{(s)}(\alpha^*,\alpha)/d\tau$ and integrate by parts the right-hand side of Eq. (A2) we get the equation of motion for $\langle \alpha^{*m}\alpha^n\rangle_{(s)}$. The second truncation means that we restrict ourselves only to the set of equations for the first- and second-order statistical moments $\langle\alpha\rangle_{(s)}$, $\langle\alpha^*\alpha\rangle_{(s)}$, and $\langle\alpha^2\rangle_{(s)}$. We have

$$\frac{d}{d\tau}\langle\alpha\rangle_{(s)}=-\tfrac{1}{2}\Gamma\langle\alpha\rangle_{(s)}+\mathcal{F}-i\langle\alpha^*\alpha^2\rangle_{(s)}+i(1-s)\langle\alpha\rangle_{(s)}\ , \tag{A3}$$

$$\frac{d}{d\tau}\langle\alpha^2\rangle_{(s)}=-\Gamma\langle\alpha^2\rangle_{(s)}+2\mathcal{F}\langle\alpha\rangle_{(s)}-2i\langle\alpha^*\alpha^3\rangle_{(s)}+i(2-3s)\langle\alpha^2\rangle_{(s)}\ , \tag{A4}$$

$$\frac{d}{d\tau}\langle\alpha^*\alpha\rangle_{(s)}=-\Gamma\langle\alpha^*\alpha\rangle_{(s)}+\mathcal{F}[\langle\alpha\rangle_{(s)}+\langle\alpha^*\rangle_{(s)}]+\Gamma\left[\langle n\rangle+\frac{(1-s)}{2}\right]\ . \tag{A5}$$

We see that the right-hand sides of Eqs. (A3)–(A5) contain the statistical moments higher than second order. To get Eqs. (A3)–(A5) in a closed form we have to express these moments as functions of the first- and second-order moments. We substitute

$$\langle\alpha^*\alpha^2\rangle_{(s)}=2\xi B_{(s)}+\xi^*C+\xi^2\xi^*\ , \tag{A6}$$

$$\langle\alpha^*\alpha^3\rangle_{(s)}=3\xi^2B_{(s)}+3B_{(s)}C+3\xi^*\xi C+\xi^*\xi^3\ . \tag{A7}$$

The cumulants ξ, $B_{(s)}$, and C are defined by (14), (15), and (16), respectively. The relations (A6)–(A7) can be formally derived as follows [3,18]:

$$\langle\alpha^{*m}\alpha^n\rangle_{(s)}=\frac{\partial^{m+n}}{\partial(-\beta^*)^n\partial\beta^m}C_{(s)}(\beta^*,\beta)|_{\beta=\beta^*=0}\ , \tag{A8}$$

where $C_{(s)}(\beta^*,\beta)$ is the quantum characteristic function related to s ordering:

$$C_{(s)}(\beta^*,\beta)=\exp[-\beta^*\beta B_{(s)}+\tfrac{1}{2}\beta^{*2}C+\tfrac{1}{2}\beta^2C^*-\beta^*\xi+\beta\xi^*]\ . \tag{A9}$$

To get Eq. (17) we substitute Eq. (14) and Eq. (A6) into Eq. (A3). We have

$$\frac{d\xi}{d\tau}=-\frac{1}{2}\Gamma\xi+\mathcal{F}-i\left[2\left[B_{(s)}-\frac{1-s}{2}\right]\xi+C\xi^*+\xi^2\xi^*\right]\ . \tag{A10}$$

On substituting $G_{(s)}=B_{(s)}-(1-s)/2$ into the above equation, we get Eq. (17).

In a similar way we obtain Eq. (18). First, let us note that from Eq. (16) we have

$$\frac{dC}{d\tau}=\frac{d\langle\alpha^2\rangle_{(s)}}{d\tau}-2\langle\alpha\rangle_{(s)}\frac{d\langle\alpha\rangle_{(s)}}{d\tau}\ . \tag{A11}$$

Second, we insert Eqs. (A3) and (A4) into Eq. (A11) and after some mathematics we get

$$\frac{dC}{d\tau}=-\Gamma C-i\xi^2\left[1+2\left[B_{(s)}-\frac{1-s}{2}\right]\right]+iC(1+4|\xi|^2)-6i\left[B_{(s)}-\frac{1-s}{2}\right]C\ . \tag{A12}$$

Taking into account that $G_{(s)}=B_{(s)}-(1-s)/2$ we immediately get Eq. (18).

To obtain Eq. (19) we note that from Eq. (15) we have

$$\frac{dB_{(s)}}{d\tau}=\frac{d\langle\alpha^*\alpha\rangle_{(s)}}{d\tau}-\frac{d\langle\alpha^*\rangle_{(s)}}{d\tau}\langle\alpha\rangle_{(s)} -\langle\alpha^*\rangle_{(s)}\frac{d\langle\alpha\rangle_{(s)}}{d\tau} . \tag{A13}$$

On substituting Eq. (A5) and Eq. (A3) into Eq. (A13) we get

$$\frac{dB_{(s)}}{d\tau}=-\Gamma\left[B_{(s)}-\frac{1-s}{2}\right]+i(C\xi^{*2}-C^*\xi^2)+\Gamma\langle n\rangle . \tag{A14}$$

On substituting $G_{(s)}=B_{(s)}-(1-s)/2$ we obtain Eq. (19).

[1] G. Casati and L. Molnari, Prog. Theor. Phys. **98**, 287 (1989).

[2] J. H. Jensen and Q. Niu, Phys. Rev. A **42**, 2513 (1990).

[3] J. Peřina, *Quantum Statistics of Linear and Nonlinear Optical Phenomena* (Reidel, Dordrecht, 1984).

[4] M. V. Berry, in *Chaotic Behavior of Deterministic Systems*, 1981 Les Houches Lectures, edited by G. Iooss, R. H. G. Helleman, and R. Stora (North-Holland, Amsterdam, 1983).

[5] K. Vogel and H. Risken, Phys. Rev. A **38**, 2409 (1988).

[6] G. P. Berman and G. M. Zaslavsky, Physica **111A**, 17 (1982).

[7] G. J. Milburn, Phys. Rev. A **33**, 674 (1986).

[8] G. J. Milburn and C. A. Holms, Phys. Rev. Lett. **56**, 2237 (1986).

[9] V. Peřinová and A. Lukš, Phys. Rev. A **41**, 414 (1990).

[10] V. Peřinová and A. Lukš, J. Mod. Opt. **35**, 1513 (1988).

[11] W. H. Louisell, *Quantum Statistical Properties of Radiation* (Wiley, New York, 1973).

[12] A. Wolf, J. B. Swift, H. L. Swinney, and J. A. Vastano, Physica D **16**, 285 (1985).

[13] K. Grygiel and P. Szlachetka, Opt. Commun. **91**, 241 (1992). The Lyapunov spectrum in nonautonomous version for a system of second-harmonic generation of light with a train of pulses has been presented.

[14] K. Grygiel and P. Szlachetka (unpublished). There is a difference between the Lyapunov spectrum for a purely autonomous system and an autonomized system. For example, in a three-dimensional purely autonomous dissipative system we can observe only the following possible Lyapunov spectra $\{\lambda_1,\lambda_2,\lambda_3\}$: a chaotic attractor $\{+,0,-\}$; a quasiperiodic orbit $\{0,0,-\}$; a limit cycle $\{0,-,-\}$; and a fixed point $\{-,-,-\}$. In a three-dimensional autonomized system, i.e., a system which arises from a two-dimensional nonautonomous system, the spectrum is of the type $\{\lambda_1,\lambda_2,0\}$. See also H. Haken, Phys. Lett. A **94**, 71 (1983).

[15] R. F. Pawula, Phys. Rev. **162**, 186 (1967).

[16] J. Marcinkiewicz, Math. Z. **44**, 612 (1939).

[17] J. Ford and M. Ilg, Phys. Rev. A **45**, 6165 (1992).

[18] It has been proved by Schack and Schenzle, Phys. Rev. A **41**, 3847 (1990), that only the second-order cumulants, that is, B_s, are dependent on the ordering parameter s.